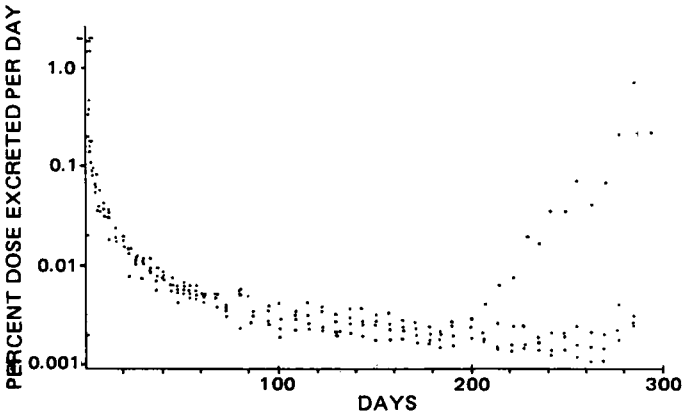

Figure 2—*Rate of fecal excretion of ^{14}C-radioactivity after subcutaneous injection of poly(methyl [1-^{14}C]methacrylate) nanoparticles into rats (n = 4).*

servation of a lag phase for the elimination of implanted material is not new. In 1955, Oppenheimer *et al.* (8) observed a lag period of 54 weeks after implantation of poly(methyl [1-^{14}C]methacrylate) films into rats, until suddenly the excretion of radioactivity started and continued for 40 weeks. When the films were removed, the excretion of radioactivity disappeared. Schindler *et al.* (13) observed with polylactide implants that degradation of the polymer, measured by the decrease in the molecular weight *via* the viscosity of the implant, started soon after administration. The removal of material from the administration site, however, occurred only after a certain molecular weight was reached. After implantation of poly(ε-caprolactone-co-DL-lactic acid) capsules for instance, the viscosity decreased by 75%, while only 1% of the injected capsule material was removed from the injection site. Since the viscosity is directly related to the molecular weight, a comparable reduction of ~75% in the molecular weight has to be assumed. Over the following 8 weeks, the residual polymer disappeared totally from the site of administration, while the viscosity decreased only slowly.

A similar process possibly occurred after subcutaneous administration of poly(methyl [1-^{14}C]methacrylate) nanoparticles and films. The degradation might have started rather early after injection or implantation, but the removal from the site of administration and the excretion began only when a certain molecular weight of the degradation products was reached. The faster excretion rate during the first couple of days can also be explained by the limitation of the transportation and excretion process by the molecular weight. The initially excreted total amount of ~13% far exceeds the possible amount of residual monomers. As mentioned previously, ≤1% residual monomers are contained in the polymer. However, as shown by gel permeation chromatography (14), the molecular weight distribution of the poly(methyl [1-^{14}C]methacrylate) nanoparticles prepared by γ-irradiation is rather wide, allowing for a considerable amount of low-molecular weight polymer, some of which could be readily excreted.

REFERENCES

(1) J. Kreuter and P. P. Speiser, *Infect. Immun.*, **13**, 204 (1976).

(2) J. Kreuter, R. Mauler, H. Gruschkau, and P. P. Speiser, *Exp. Cell Biol.*, **44**, 12 (1976).

(3) J. Kreuter and E. Liehl, *Med. Microbiol. Immunol.*, **165**, 111 (1978).

(4) J. Kreuter and E. Liehl, *J. Pharm. Sci.*, **70**, 367 (1981).

(5) J. Kreuter and I. Haenzel, *Infect. Immun.*, **19**, 667 (1978).

(6) J. Kreuter, U. Täuber, and V. Illi, *J. Pharm. Sci.*, **68**, 1443 (1979).

(7) L. Tomatis, *Tumori*, **52**, 165 (1966).

(8) B. S. Oppenheimer, E. T. Oppenheimer, I. Danishefsky, A. P. Stout, and F. R. Eirich, *Cancer Res.*, **15**, 333 (1955).

(9) A. Murray and D. L. Williams, "Organic Synthesis with Isotopes, Part I," Interscience, New York, N.Y., 1958.

(10) P. Edman and I. Sjöholm, *J. Pharm. Sci.*, **70**, 684 (1981).

(11) M. Barvic, K. Kliment, and M. Zaradil, *J. Biomed. Mater. Res.*, **1**, 313 (1967).

(12) L. Sprincl, J. Kopecek, and D. Lim, *J. Biomed. Mater. Res.*, **4**, 447 (1971).

(13) A. Schindler, R. Jeffcoat, G. L. Kimmel, C. G. Pitt, M. E. Wall, and R. Zweidinger, in "Contemporary Topics in Polymer Science," Vol. 2, E. M. Pearce and J. F. Schaefgen, Eds., Plenum, New York, N.Y., 1977, pp. 251–289.

(14) V. Bentele, U. E. Berg, and J. Kreuter, *Int. J. Pharm.* **13**, 109 (1983).

Solid-State Decomposition of Alkoxyfuroic Acids in the Presence of Microcrystalline Cellulose

J. T. CARSTENSEN ˣ and ROHIT C. KOTHARI *

Received April 9, 1982, from the *School of Pharmacy, University of Wisconsin, Madison, WI 53706.* Accepted for publication August 24, 1982. * Present address: Riker Laboratories, St. Paul, MN 55119.

Abstract □ A solid–solid interaction between alkoxyfuroic acids and microcrystalline cellulose has been studied. The decomposition of the mixture differs from that of the drug(s) alone, in that carbon monoxide (not carbon dioxide) is the high-temperature decomposition product. A model is proposed in which interaction occurs at contact points. A liquid decomposition product, dissolving part of the alkoxyfuroic acid (to the extent of its solubility) serves as a carrier, so that the number of contact points increases, thus accelerating the reaction. Both the main and ancillary parameters have calculated values that are consistent with the model.

Keyphrases □ Alkoxyfuroic acid—solid-state interactions with microcrystalline cellulose, decomposition model □ Microcrystalline cellulose—solid-state interactions with alkoxyfuroic acids, decomposition model □ Decomposition—alkoxyfuroic acids with microcrystalline cellulose, model, solid-state interactions

The interaction between solid drugs and solid excipients is of great theoretical and practical interest. Most studies deal with multicomponent systems, but even when only two solid components are present, the presence of air complicates the interpretation of data. Nevertheless, good direct conclusions have frequently been derived (1, 2).

This study describes the interaction between a drug (5-alkyloxy-2-furoic acid)[1] and a common pharmaceutical excipient (microcrystalline cellulose). Interactions between drugs and this excipient have been reported in the past (3) and present a challenging field of investigation.

EXPERIMENTAL

The 5-alkoxy-2-furoic acids were synthesized and purified as described by Carstensen and Kothari (4). The microcrystalline cellulose used[2] was

[1] A few studies were carried out with the C_8 derivative as well.

[2] Avicel; FMC Corp., West Point, Pa.

0022-3549/83/1000-1149$01.00/0
© 1983, American Pharmaceutical Association

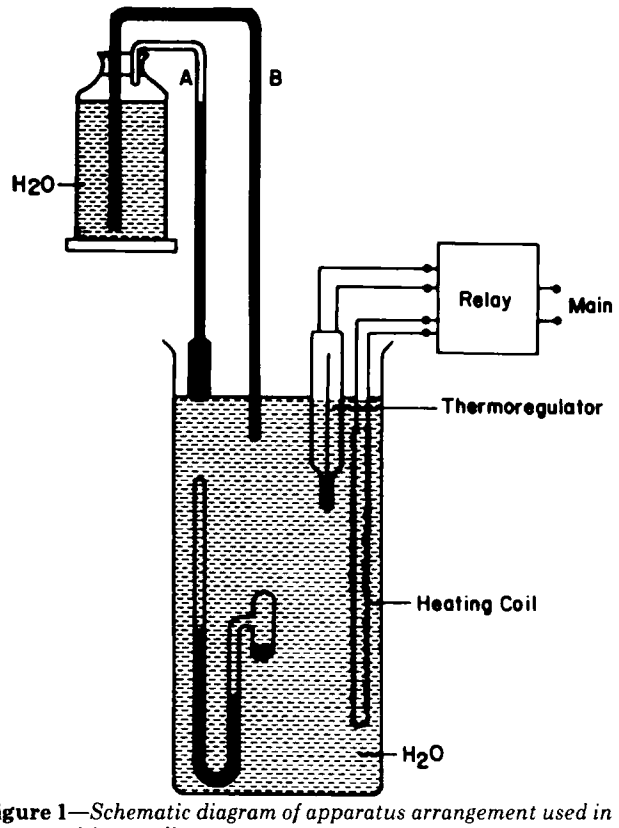

Figure 1—*Schematic diagram of apparatus arrangement used in the decomposition studies.*

found to contain 3% water as determined by (*a*) use of a vacuum electrobalance and (*b*) Karl Fischer titration. To eliminate the effect of water, the microcrystalline cellulose was dried *in vacuo* on a high-vacuum rack for 10 hr just prior to the preparation of the sample for kinetic studies.

The kinetic studies were carried out by mixing furoic acid with microcrystalline cellulose (see below) and placing the powder mixture in the sidearm of a fused manometer as described by Carstensen and Kothari (5). This was then placed in a constant-temperature bath as shown in Fig. 1, and the level of the mercury was determined as a function of time. The volumes of sample bulb and of the high-pressure side of the manometer (as a function of level) were determined as described by Carstensen and Musa (6). Knowledge of the density of mercury at the temperature in question allows conversion of mercury level to pressure, and hence the number of moles of gas produced can be calculated by means of the ideal gas law.

Although the decomposition of the two solids takes place in the absence of air, there is mercury vapor in the atmosphere above the solids which has been shown to effect some systems (7). The decomposition was, therefore, carried out in breakseal tubes (7) for certain samples. In a breakseal tube sample there is no mercury vapor in the head space. No significant difference was observed in decomposition rates, so that, unless otherwise noted, the studies were done in the fused manometer as shown in Fig. 1.

Since intimacy of mixing is important, a variety of mixing methods were tested:

1. Physical mixtures of the two compounds were made in various proportions and were mixed using a quartering technique. Some samples were ground in a ball mill. The ratios used are shown in Table I.

2. The alkoxyfuroic acid was weighed and dissolved in a solvent (methanol or acetone). Weighed amounts of microcrystalline cellulose were then added, and the suspension was stored in a closed container for 12 hr. The solvent was evaporated and then the samples were tested by the fused manometer and breakseal techniques. The surface area of the samples was tested by krypton adsorption[3]. The Brunauer–Emmett–Teller equation (8) was used for calculation of the surface from the adsorption data.

The gas evolved was carbon monoxide (not carbon dioxide) at elevated temperatures[4]. This identification was carried out in two ways. At the end of the kinetic study the sample bulb was immersed in a toluene slush (9) in a Dewar flask. The toluene slush (a mixture of ~80% solid toluene and 20% liquid toluene at the melting point of toluene, 178°K) was prepared by adding liquid nitrogen to toluene in a Dewar flask while stirring the liquid. The toluene eventually started freezing, and addition of liquid nitrogen was stopped when a "slush" was obtained giving a constant temperature reservoir as long as solid toluene was present. If the evolved gas is condensable at 178°K (*e.g.*, carbon dioxide), then the gas in the head space should condense and the pressure in the manometer equilibrate to zero. The gas, however, was not condensable at 178°K. Samples of the head space gas were analyzed by MS and identified as carbon monoxide.

[3] Quantasorb; Quantachrome Corp. Syosset, NY 11791.

[4] The conclusions refer to the temperatures used here only. It is doubtful that measurable amounts of carbon monoxide would be formed at room temperature.

Table I—Statistical Comparison of the Models According to Eqs. 1A, 2, and 3A

Derivative[a]	Furoic Acid, %	Temperature	s^2_{yx} for Model		
			Eq. 2	Eq. 3A	Eq. 1A
C_{14}	60	90°	0.00234	0.00380	0.00106
C_{14}	40[b]	90°	0.00159	0.00956	0.00006
C_{14}	80	90°	0.00143	0.00457	0.00004
C_{14}	40	90°	0.00027	0.00025	0.00008
C_{14}	20[b]	90°	0.00093	0.01230	0.00014
C_{14}	20	90°	0.00018	0.00333	0.00125
C_{14}	10	90°	0.00000	0.00192	0.00001
C_{14}	30[c]	90°	0.00197	0.00321	0.00000
C_{14}	47[c]	90°	0.01132	0.02179	0.00189
C_{14}	18[c]	90°	0.00016	0.00238	0.00051
C_{14}	40[d]	90°	0.00140	0.00639	0.00004
C_{14}	20[d]	90°	0.00002	0.00232	0.00000
C_8	20	90°	0.00000	0.00145	0.00000
C_8	40	90°	0.00016	0.00033	0.00003

[a] Number of side-chain carbons. [b] Ground in ball mill. [c] Applied as a methanolic solution. [d] Applied as a solution in acetone.

RESULTS AND DISCUSSION

A typical pattern of decomposition of alkoxyfuroic acid in the presence of microcrystalline cellulose is shown in Fig. 2. The fraction decomposed (x) as a function of time (t) is a sigmoid curve, as in the case of the pure furoic acids themselves (4). A few obvious possibilities for this are delineated below. As for the case of the pure furoic acids, the decomposition could be directed by Bawn kinetics (10) in which case:

$$\ln(1 + Ax) = Kt + c'' \qquad \text{(Eq. 1)}$$

where A, K, and c'' are constants. This model relies on decomposition

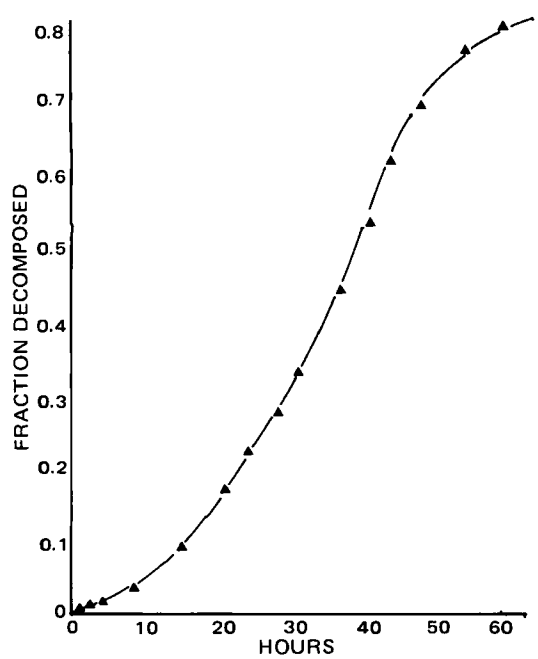

Figure 2—*Typical decomposition profile of an alkoxyfuroic acid–microcrystalline cellulose mixture, with 40% alkoxyfuroic acid (C_{18}) at 90°.*

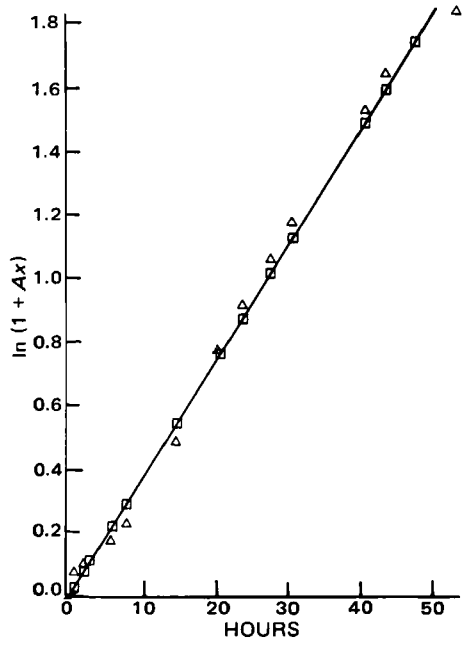

Figure 3—*Data in Fig. 2 plotted according to Eq. 1. In the ordinate,* x *is fraction decomposed and* A *(Eq. 1 and Table IV) is a floating parameter. Key: (△) = actual values; (□) = values according to least-squares fit.*

of the furoic acid in the solid state as well as in solution of the furoic acid in its (liquid) decomposition product. There is also the possibility that the decomposition occurs *via* the vapor phase, which results in zero-order kinetics (11), *i.e.*:

$$x = kt + c \qquad \text{(Eq. 2)}$$

where k and c are constants. That this is not the case is graphically obvious (Fig. 2), but it has been included as a possibility in the statistical evaluation in Table I. Finally, there is the possibility of Prout–Tompkins-type kinetics (12) where:

$$\ln|x/(1-x)| = -k't + c' \qquad \text{(Eq. 3)}$$

Unlike the decomposition of the pure furoic acids, the presence of a liquid phase was not visually obvious. This, however, could be due to adsorptive and absorptive properties of the microcrystalline cellulose. For decompositions where a solid decomposes to a solid plus a gas, Eq. 3 could be expected to hold.

For the sake of comparison, least-squares fits were performed of all data according to the three equations, and the residual sum of squares (s_{yx}^2) calculated for fits *via* Eq. 2 and from Eqs. 1 and 3 in the forms:

$$x = \exp(Kt + c'') - 1 \qquad \text{(Eq. 1A)}$$

$$x = \exp(-k't + c')/\{1 + \exp(-k't + c')\} \qquad \text{(Eq. 3A)}$$

In this manner the values of s_{yx}^2 are comparable (being in the same dimensionless unit). It is obvious from Table I (Fig. 3) that Eq. 1 (Eq. 1A) fits the data better than the two other equations. Values of K and c from the various mixtures of furoic acid and microcrystalline cellulose studied are shown in Table II. For reasons that will be dealt with later, these evaluations were carried out only through 80% of the decomposition. Beyond this point there was distinct deviation from all three models.

Solid-state interactions have been covered in the past in descriptive and qualitative fashions (13–15), but in a quantitative sense physical models of interactions between two solids have only occurred infrequently in the literature (16, 17). In the following an explanation for the kinetic scheme is sought using models. The first point to notice is that the decomposition of the furoic acids (RCOOH) differs when microcrystalline cellulose (R'CHOHR") is present. Furoic acids alone decompose in the following manner:

$$\text{RCOOH} \rightarrow \text{RH(liquid)} + \text{CO}_2\text{(gas)} \qquad \text{(Eq. 4)}$$

i.e., carbon dioxide is formed. Part of the decomposition occurs in the solid RCOOH and part in a saturated solution of RCOOH in RH. In the presence of microcrystalline cellulose, however, carbon monoxide is

Table II—Parameter Values for Decomposition of Furoic Acids in Contact With Microcrystalline Cellulose [a]

Derivative	Furoic Acid, %	Temperature	$\ln(1+Ax) = Kt + c''$ Slope (K or q)	Intercept (c'')	R^2 [b]
C_{14}	60	90°	0.066	−0.0008	0.98
C_{14}	40[c]	90°	0.057	0.00009	0.97
C_{14}	80	90°	0.035	0.00002	0.98
C_{14}	40	90°	0.036	0.00008	0.99
C_{14}	20[d]	90°	0.107	0.00010	0.99
C_{14}	20	90°	0.049	−0.00005	0.97
C_{14}	30[e]	90°	0.043	−0.00001	0.98
C_{14}	10	90°	0.016	0.00005	0.99
C_{14}	47[e]	90°	0.042	0.00004	0.93
C_{14}	18[e]	90°	0.008	0.00000	0.97
C_{14}	40[f]	90°	0.017	−0.00004	0.99
C_{14}	20[f]	90°	0.013	0.00007	0.99
C_8	20	90°	0.004	−0.00001	0.99
C_8	40	90°	0.016	−0.00002	0.99
C_{14}	40	85°	0.0039	−0.06168	0.98
C_{14}	40	95°	0.0688	−0.01793	0.99
C_{14}	40	100°	0.5836	0.02268	0.99

[a] Data treated according to Eq. 1. [b] Correlation coefficient squared. [c] Ground in ball mill. [d] Hand ground with a mortar and pestle. [e] Applied as a methanolic solution. [f] Applied as a solution in acetone.

formed. Without any kind of speculation as to the actual interaction between the two solids, it may be stated generally that:

$$\text{RCOOH} + \text{R'CHOHR''} \rightarrow \text{Q}_1 + \text{Q}_2 + \text{CO} \qquad \text{(Eq. 5)}$$

where Q_1 and Q_2 are decomposition products. One of these (or both of them) could be liquid.

Cellulose, of course, decomposes at elevated temperatures, but usually not until >140° (18) within the time periods used in this study. The usual decomposition path is one of loss of water, leading to the formation of dehydrocellulose.

It is possible to visualize reaction schemes including microcrystalline cellulose, such as:

$$\text{RCOOH} + \text{R'CHOHR''} \rightarrow \text{RH} + \text{CO} + \text{H}_2\text{O} + \text{R'(C:O)R''} \qquad \text{(Eq. 6)}$$

where RH is liquid. It is also possible to visualize schemes where the microcrystalline cellulose does not take part in the overall reaction, *i.e.*, where it serves as a catalyst:

$$\text{RCOOH(+ R'CHOHR'')} \rightarrow \text{ROH} + \text{CO(+ R'CHOHR'')} \qquad \text{(Eq. 7)}$$

It should be pointed out that neither of these two schemes have been substantiated, and they are mentioned solely to show that reactions of the type in Eq. 5 are feasible stoichiometrically.

At first thought, reactions such as Eqs. 4 and 5 would not seem to differ widely. RCOOH could dissolve in Q_1 and justify the Bawn-type kinetics which apply to such a situation. But in that case it should not matter if the materials were ground or not. It is noted from Table II that grinding gives an increased decomposition rate (0.057 *versus* 0.036 hr^{-1} for 40% acid and 0.107 *versus* 0.049 hr^{-1} for 20% acid). Hence, contact points between the alkoxyfuroic acid and the microcrystalline cellulose must be involved. A model which accounts for this is:

1. At contact points (the number of which is denoted N in the following) a reaction of the type shown in Eq. 5 takes place giving at least one liquid decomposition product (*e.g.*, Q_1).
2. The furoic acid will dissolve in the Q_1 to the extent of its solubility (S moles per mole of Q_1) and will start covering the surface (a, cm^2) of the microcrystalline cellulose.
3. The reaction then accelerates because of increased contact points between the (now dissolved) furoic acid and the microcrystalline cellulose.
4. Due to crowding there will, eventually, be a deceleration period.

It might be argued that the external surface of the microcrystalline cellulose would be insufficient to account for the total decomposition. There are, however, two "types" of surface present in microcrystalline cellulose: nitrogen adsorption gives low surface areas, whereas water isotherms give surface areas 100 times as large (19–22).

By the decomposition at a contact point, it is assumed that the decomposition, creating one Q_1 molecule, will dislodge (dissolve) S molecules of RCOOH at the contact point. If the initial number of contact points is N_0 and if there is a reaction possibility of α at each contact point,

Table III—Late-Period Data Treated According to Eq. 24

Derivative	Furoic Acid, %	Temperature	$\ln(1-x) = -K't + D$ Slope ($-K'$)	Intercept (D)	R^2 [a]	$\phi L_0/N_0$
C_{14}	60	90°	−.061	1.70	0.998	1.50
C_{14}	40[b]	90°	−0.55	0.68	0.967	0.67
C_{14}	80	90°	−0.036	1.06	0.946	4.00
C_{14}	40	90°	−0.041	0.82	0.99	0.67
C_{14}	20[c]	90°	−0.037	−0.20	0.875	0.21
C_{14}	20	90°	−0.021	−0.42	0.895	0.25
C_{14}	30[d]	90°	−0.052	1.18	0.989	0.43
C_{14}	10	90°	−0.038	0.0031	0.979	0.11
C_{14}	47[d]	90°	−0.11	3.6	0.987	0.89[f]
C_{14}	18[d]	90°	−0.017	−0.16	0.943	0.22
C_{14}	40[e]	90°	−0.034	1.28	0.970	0.67
C_{14}	20[e]	90°	−0.038	0.97	0.999	0.25
C_8	20	90°	−0.020	0.60	0.998	
C_8	40	90°	−0.016	0.44	0.955	
C_{14}	40	85°	−0.010	1.23	0.995	
C_{14}	40	95°	−0.081	1.51	0.993	
C_{14}	40	100°	−0.39	1.05	0.984	

[a] Coefficient of correlation squared. [b] Ground in ball mill. [c] Hand ground with a mortar and pestle. [d] Applied as a methanolic solution. [e] Applied as a solution in acetone. [f] Data not included in D *versus* $\phi L_0/N_0$ correlation.

then:

$$dN/dt = \alpha \cdot (S-1) \cdot N \qquad \text{(Eq. 8)}$$

since, when α molecules react, $\alpha \cdot S$ new contact points are created, and one (the one at which the reaction takes place) is lost.

At some point in time there will arise the distinct probability of "overcrowding," *i.e.*, saturated Q_1 will start getting in contact with sites already reacted (containing Q_2 and not native microcrystalline cellulose). If this probability is proportional to N, with proportionality constant β [similar to a termination probability in a Prout–Tompkins-type reaction (12)], then Eq. 8 becomes:

$$dN/dt = q \cdot N \qquad \text{(Eq. 9)}$$

where:

$$q = \alpha \cdot (S-1) - \beta \qquad \text{(Eq. 10)}$$

There would be an initial value of α denoted α_0, and initially the value of β would be zero. In Prout–Tompkins reactions it takes considerable time before β becomes sizable. However, in the model proposed here, the external surface is relatively small (compared with the total surface) so that the crowding may be assumed to occur rapidly, and if it is assumed that β has a finite value from the onset, then considering $\alpha = \alpha_0$ and $\beta = \beta_0$ throughout the process may be acceptable. This allows integration of Eq. 9, which with imposition of initial conditions yields:

$$N = N_0 \cdot e^{qt} \qquad \text{(Eq. 11)}$$

Since the rate of decomposition is proportional to the number of contact points at a given time t, then denoting by L the number of molecules of alkoxyfuroic acid that are intact at time t:

$$dL/dt = -\gamma \cdot N \qquad \text{(Eq. 12)}$$

where γ is a constant. From the definition of L it follows that:

$$x = (L_0 - L)/L_0 \qquad \text{(Eq. 13)}$$

This inserted in Eq. 12 yields:

$$dx/dt = -(1/L_0)dL/dt \qquad \text{(Eq. 14)}$$

which inserted in Eq. 12 gives:

$$dx/dt = (1/L_0) \cdot \gamma \cdot N \qquad \text{(Eq. 15)}$$

Substituting Eq. 11 into Eq. 15 then gives:

$$dx/dt = (\gamma N_0/L_0)e^{qt} \qquad \text{(Eq. 16)}$$

Integration of this (with imposition of initial conditions) yields:

$$x = (\gamma N_0/\{L_0 q\})(e^{qt} - 1) \qquad \text{(Eq. 17)}$$

If:

$$A = \{L_0 q/(\gamma N_0)\} \qquad \text{(Eq. 18)}$$

then the logarithmic form of Eq. 18 is identical to the Bawn equation (Eq. 1):

$$\ln(1 + Ax) = qt \qquad \text{(Eq. 19)}$$

Eq. 19 differs from Eq. 1 in the sense that the intercept is zero. It is seen from Table II, that this indeed is the case: all the intercepts listed fail to differ significantly from zero. q is hence equal to K in Eq. 1 (Table II).

Even though Eq. 19 is of the general form of a Bawn equation, the argumentation leading to its derivation is quite different. The fact that the data fit Eq. 19 is no proof of the proposed model. In fact, a model can never be proven correct, one can only fail to show that it contradicts a particular set of data, and this, in itself, does not guarantee that other models (not thought of) might not prove to be better. To lend credence to a model it is worthwhile to ascertain that it is consistent in as many respects as can be thought of.

There are two distinct cases in the aforementioned model: (*a*) the number of surface sites of the microcrystalline cellulose (N_0) is larger than the initial number of alkoxyfuroic acid molecules (L_0), or (*b*) the opposite is the case. The former (*a*) is the case in this study. In general a model has a certain domain in which it applies, and beyond which other mechanisms take over. In the case in point, there will be a given point in time, t', at which all the furoic acid will have dissolved; *i.e.*, beyond this point there is no more solid furoic acid in the system, it is all dissolved, and adsorbed at sites on the microcrystalline cellulose.

If there are L' intact furoic acid molecules left at t', then $(L_0 - L')$ molecules of Q_0 will have been formed, so that (by definition of S):

$$S = L'/(L_0 - L') \qquad \text{(Eq. 20)}$$

or:

$$L' = L_0 S/(1 + S) \qquad \text{(Eq. 21)}$$

After t' the rate of decrease in number of furoic acid molecules would simply be proportional to the number of intact furoic acid molecules, *i.e.*:

$$dL/dt = -K' \cdot L \qquad \text{(Eq. 22)}$$

since there is no longer a termination probability. (The molecules are visualized as situated at microcrystalline cellulose sites with a probability of K' of reacting.) Integrating this and imposing that $L = L'$ at $t = t'$ then gives:

$$\ln L = -K'(t - t') + \ln[SL_0/(1 + S)] \qquad \text{(Eq. 23)}$$

or:

$$(L/L_0) = (1 - x) = [S/(1 + S)] \cdot e^{-K'(t-t')} \qquad \text{(Eq. 24)}$$

The logarithmic form of this is:

$$\ln(1 - x) = -K' \cdot t + D \qquad \text{(Eq. 25)}$$

where:

$$D = K't' + \ln[S/(1 + S)] \qquad \text{(Eq. 26)}$$

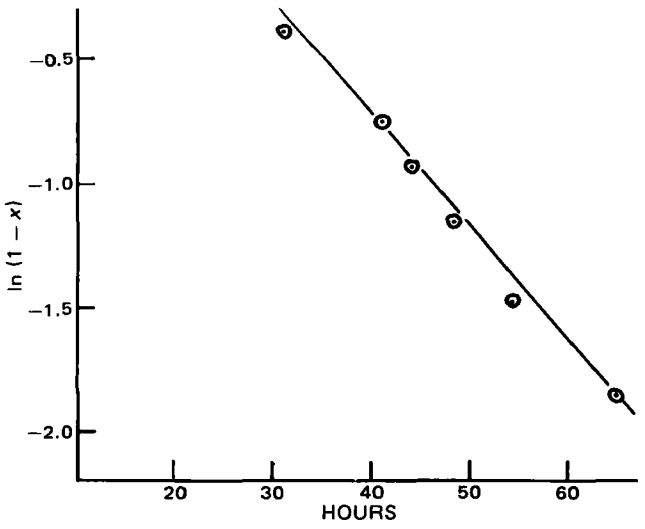

Figure 4—*The late phase of decomposition, which is supposed to be first order. ln(1 − x) is plotted* versus *time for a C_{14} alkoxyfuroic acid–microcrystalline cellulose mixture (40:60).*

Hence the latter part of the curve should be an exponential decay curve. Data treated in this fashion are shown in Fig. 4, and least-squares fit values are shown in Table III.

Precision in this range is, of course, less than the remainder of the data, since all the x values are between 0.8 and 1.0. Nevertheless fits are good (as judged by visual inspection of the figure, as well as from correlation coefficients in the table).

At a particular temperature, the solubility S is constant. It is noted that at time t' (Eq. 17):

$$(L_0 - L')/L_0 = x' = \{\gamma N_0/(L_0 q)\} \cdot (e^{qt'} - 1) \qquad \text{(Eq. 27)}$$

This may be rearranged to read:

$$t' = (1/q) \cdot \{1 + \ln[(L_0 - L') \cdot q/(\gamma \cdot N_0)]\} \sim (1/q) \cdot \ln(L_0/N_0) + (1/q) \cdot \ln(q/\gamma) \qquad \text{(Eq. 28)}$$

where the approximation $e^{qt'} \gg 1$[5] and $L' \ll L_0$. N_0 is proportional to the amount of microcrystalline cellulose (M_1,g) and L_0 is proportional to the amount of furoic acid (M_0,g). Hence (L_0/N_0) is proportional to M_2/M_1, *i.e.*:

$$M_2/M_1 = \phi \cdot (L_0/N_0) \qquad \text{(Eq. 29)}$$

where ϕ is a constant. When Eqs. 28 and 29 are inserted in Eq. 26, the following expression emerges:

$$D = (K'/q)[(\ln(M_2/M_1) - \ln q + \ln(\gamma\phi)] + \ln(S/\{1 + S\}) \qquad \text{(Eq. 30)}$$

If S is sizable (as in the case of the pure furoic acids), then $\ln\{S/(1 + S)\}$ is approximately zero, so that Eq. 29, may be written (in rearranged form):

$$(D \cdot q/K') - \ln q = \ln(M_2/M_1) + \ln(\gamma\phi) \qquad \text{(Eq. 31)}$$

A plot of $(D \cdot q/K') - \ln q$ as a function of $\ln(M_2/M_1)$ should therefore be linear. The values of these two parameters are shown in Table IV, and a plot according to Eq. 31 is shown in Fig. 5. It should again be stressed that the extraction of information from the data at this point is at the limit of precision, but that it is done to check the model for consistency, not to obtain values of parameters. It is seen from Fig. 5 that a fairly good straight line ensues. The least-squares fit is:

$$(D \cdot q/K') - \ln q = 0.7 \ln(M_2/M_1) + 3.9 \qquad \text{(Eq. 32)}$$

The 95% confidence limits on the slope are ± 0.4, so that 1.0 is in this interval, hence Eq. 31 is not contradicted. Aside from operating at the limit of precision, the confidence limits on the slope are large because only five points are involved. In this treatment the milled samples were omitted for reasons mentioned earlier, and the solvent-deposited samples were omitted as well, because they appear to give lower rate constants

[5] For the data in Fig. 3, for instance, $q = 0.036$ and $t' = 50$ so that $\exp(qt') = 6$.

Table IV—ln A as a Function of $\ln(qM_2/M_1)$ [a]

Derivative	Furoic Acid, %	M_2/M_1	A	ln A	$\ln(qM_2/M_1)$
C_{14}	60	1.50	28.25	3.34	−2.31
C_{14}	40[b]	0.67	7.85	2.06	−3.27
C_{14}	80	4.00	10.75	2.37	−1.97
C_{14}	40	0.67	6.75	1.91	−3.72
C_{14}	20[c]	0.25	15.09	2.71	−3.62
C_{14}	20	0.25	5.65	1.73	−4.40
C_{14}	30[d]	0.43	9.11	2.21	−3.99
C_{14}	10	0.11	0.86	−0.15	−6.34
C_{14}	47[d]	0.90	10.66	2.37	−3.28
C_{14}	18[d]	0.23	0.86	−0.15	−6.30
C_{14}	40[e]	0.67	3.87	1.35	−4.48
C_{14}	20[e]	0.25	1.62	0.48	−5.73

[a] Data treated according to Eq. 31, least-squares fit: $\ln A = 0.73 \cdot \ln(qM_2/M_1) + 4.68$ with a correlation coefficient of 0.93. [b] Ground with a ball mill. [c] Hand ground with a mortar and pestle. [d] Applied as a methanolic solution. [e] Applied as a solution in acetone.

as shown in Table II (0.13 *versus* 0.049 hr^{-1} for 20% acid in acetone, 0.017 *versus* 0.036 hr^{-1} for 40% acid in acetone, and 0.042 *versus* a prorated 0.046 for 47% acid in methanol).

A further consistency check exists in the following consideration: Eq. 18 suggests that the parameter A in Eq. 19 (listed in Table III) should be proportional to q and to the ratio M_2/M_1. In logarithmic form Eq. 18 becomes:

$$\ln A = \ln(qL_0/N_0) - \ln\gamma = \ln(qM_2/M_1) - \ln(\phi/\gamma) \qquad \text{(Eq. 33)}$$

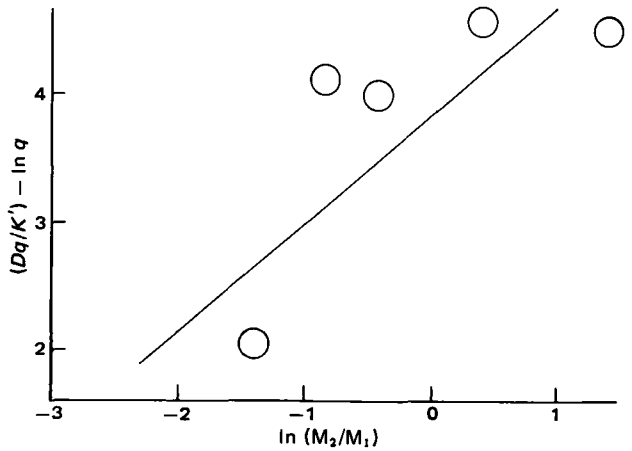

Figure 5—*Eq. 31 may be written: (Dq/K′) = ln (qM₂/M₁) + ln(φγ); the data from Table IV are presented in this fashion. Data from Table IV plotted according to Eq. 31.*

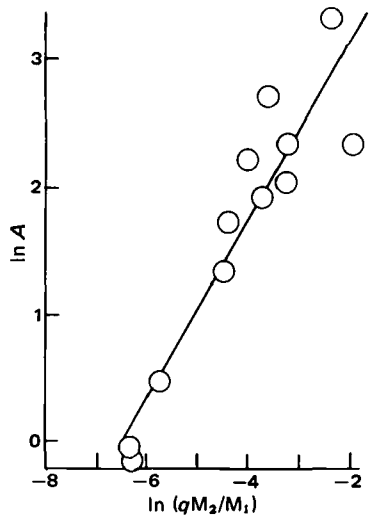

Figure 6—*The floating parameter, A, according to Eq. 33 should be a linear function of ln(qM₂/M₁); the data from Table IV are shown in this fashion.*

Table V—Temperature Dependence of K Values of C_{14} Derivative–Microcrystalline Cellulose Mixtures [a]

Temperature	1000/T	K (q)	ln K(ln q)	K'	ln K'
85°	2.792	0.0039	−5.55	0.0104	−4.56
90°	2.754	0.0360	−3.32	0.0405	−3.21
95°	2.716	0.0688	−2.67	0.0807	−2.52
100°	2.680	0.5836	−0.54	0.3940	−0.93

[a] Least-squares fit according to Eq. 33 for $K(q)$ $R^2 = -0.980$, slope = −41.88, and intercept = 111.55; for K', $R^2 = -0.989$, slope = −30.92, and intercept = 81.77.

where Eq. 30 has been introduced for the last step. Values of q are found in Table II, and values of $\ln(qM_2/M_1)$ are listed in the last column of Table III. A plot according to Eq. 33 is shown in Fig. 6. Linearity is plausible from the figure, and the correlation coefficient (0.93) is of satisfactory magnitude. The least-squares fit equation is:

$$\ln A = 0.73 \ln(qM_2/M_1) + 4.68 \qquad \text{(Eq. 34)}$$

The slope, again, does not differ significantly from unity. The values of (ϕ-γ) from Figs. 5 and 6 should be identical but as shown they differ, but (*a*) there is no actual value in obtaining the figures (other than ascertaining that they are of reasonable orders of magnitude), and (*b*) it should be stressed again, that they are obtained at the limit of precision. The restraints on ϕ and γ are that ϕ be positive and (from the argumentation leading to Eq. 12) that γ be between zero and one. The consequences of the model and the data, therefore, do not lead to contradiction in this respect either.

As a final check, the temperature dependence of the K and K' values is according to an Arrhenius equation, *i.e.*:

$$\ln K = -(E_a/R)(1/T) + \ln Z \qquad \text{(Eq. 35)}$$

where E_a is activation energy, R the gas constant, T the absolute temperature, and Z a collision factor. One composition was tested at four temperatures; the data are shown in Table V and graphically in Fig. 7. The least-squares fit parameters of these data according to Eq. 33 are shown as well. The values of E_a are 5.0 and 3.72 kJ/mole, respectively. These values are much lower than for the pure compound and are in the range expected for solution kinetics and chemisorption.

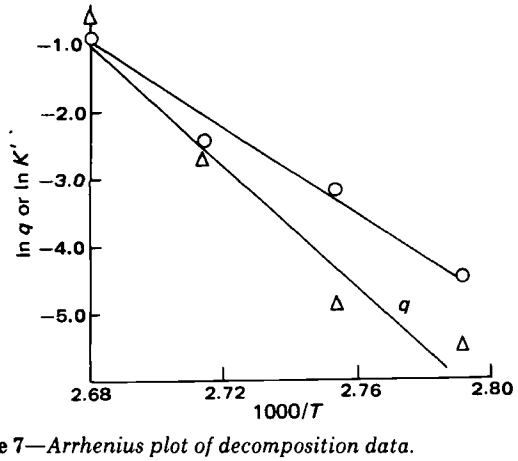

Figure 7—*Arrhenius plot of decomposition data.*

CONCLUSIONS

If microcrystalline cellulose is mixed with an alkoxyfuroic acid, an interaction takes place that could result from a direct reaction of the two components. A liquid decomposition product is formed and this serves as a carrier to increase the number of contact points and (as long as solid alkoxyfuroic acid is present) accelerate the reaction. Once all solid alkoxyfuroic acid is dissolved, the reaction becomes a reaction of adsorbed alkoxyfuroic acid.

REFERENCES

(1) A. Troup and H. Mitchner, *J. Pharm. Sci.*, **53**, 375 (1964).

(2) A. Jacobs, A. Dilatush, S. Weinstein, and J. Windheuser, *J. Pharm. Sci.*, **55**, 893 (1966).

(3) J. Carstensen, M. Osadca, and S. Rubin, *J. Pharm. Sci.*, **58**, 549 (1969).

(4) J. T. Carstensen and R. Kothari, *J. Pharm. Sci.*, **70**, 1095 (1981).

(5) J. T. Carstensen and R. Kothari, *J. Pharm. Sci.*, **69**, 123 (1980).

(6) J. T. Carstensen and M. N. Musa, *J. Pharm. Sci.*, **61**, 1112 (1972).

(7) J. T. Carstensen and P. Pothisiri, *J. Pharm. Sci.*, **64**, 37 (1975).

(8) S. Brunauer, P. Emmett, and E. Teller, *J. Am. Chem. Soc.*, **60**, 309 (1938).

(9) J. T. Carstensen, "Radiolysis of Gaseous Ammonia," Ph.D. Thesis Stevens Institute of Technology, 1967.

(10) C. E. H. Bawn, in "Chemistry of the Solid State," W. E. Garner, Ed., Butterworths, London, England, 1955, p. 254.

(11) P. Pothisiri and J. T. Carstensen, *J. Pharm. Sci.*, **64**, 1931 (1975).

(12) E. G. Prout and F. C. Tompkins, *Trans. Faraday Soc.*, **40**, 488 (1944).

(13) Y. Machida and T. Nagai, *Chem. Pharm. Bull.*, **22**, 2346 (1974).

(14) K. Takayama, N. Nambu, and T. Nagai, *Chem. Pharm. Bull.*, **25**, 879 (1977).

(15) K. Takayama, N. Nambu, and T. Nagai, *Chem. Pharm. Bull.*, **25**, 2608 (1977).

(16) W. Jander, *Z. Anorg. Chem.*, **163**, 1 (1927).

(17) R. P. Rastogi and N. B. Singh, *J. Phys. Chem.*, **70**, 3315 (1966).

(18) P. Burkart, J. Bandisch, and C. Ruscher, *Tappi*, **52**, 693 (1969).

(19) R. G. Hollenbeck, G. E. Peck, and D. O. Kildsig, *J. Pharm. Sci.*, **67**, 1599 (1978).

(20) K. Marshall, D. Sixsmith, and N. G. Stanley-Wood, *J. Pharm. Pharmacol.*, **24**, Suppl., 138p (1972).

(21) Y. Nakai, E. Fukuoka, S. Nakajima, and J. Hasegawa, *Chem. Pharm. Bull.*, **25**, 96, (1977).

(22) Y. Nakai, S. Nakajima, K. Yamamoto, K. Terada, and T. Konno, *Chem. Pharm. Bull.*, **28**, 652 (1980).

ACKNOWLEDGMENTS

Abstracted in part from a dissertation submitted by R. C. Kothari to the University of Wisconsin in partial fulfillment of the Doctor of Philosophy degree requirements.

Supported in part by a research grant from Hoffmann-La Roche, Inc., Nutley, NJ 07110.

The authors thank Dr. J. Sheridan, Hoffmann-La Roche, Nutley, N.J. and Drs. M. A. Zoglio and R. A. Parker, Merrell-Dow Laboratories, Cincinnati, Ohio for technical assistance.